

# Photoacoustic Spectrometer with a Calculable Cell Constant for Measurements of Gases and Aerosols<sup>†</sup>

Daniel K. Havey,<sup>\*,‡,§</sup> Pedro A. Bueno,<sup>§,||</sup> Keith A. Gillis,<sup>§</sup> Joseph T. Hodges,<sup>§</sup>  
George W. Mulholland,<sup>§,||</sup> Roger D. van Zee,<sup>§</sup> and Michael R. Zachariah<sup>§,||</sup>

Department of Chemistry and Biochemistry, James Madison University, MSC 4501, Harrisonburg, Virginia 22807, Chemical Science and Technology Laboratory, National Institute of Standards and Technology, 100 Bureau Drive, Gaithersburg, Maryland 20899, and Department of Mechanical Engineering and Department of Chemistry and Biochemistry, University of Maryland, College Park, Maryland 20742

We benchmark the performance of a photoacoustic spectrometer with a calculable cell constant in applications related to climate change measurements. As presently implemented, this spectrometer has a detection limit of  $3.1 \times 10^{-9} \text{ W cm}^{-1} \text{ Hz}^{-1/2}$  for absorption by a gas and  $1.5 \times 10^{-8} \text{ W cm}^{-1} \text{ Hz}^{-1/2}$  for soot particles. Non-statistical uncertainty limited the accuracy of the instrument to  $\sim 1\%$ , and measurements of the concentration of  $\text{CO}_2$  in laboratory air agreed with measurements made using a cavity ring-down spectrometer, to within 1%. Measurements of the enhanced absorption resulting from ultrathin ( $< 5 \text{ nm}$ ), nonabsorbing coatings on nanoscale soot particles demonstrate the sensitivity of this instrument. Together, these measurements show the instrument's ability to quantitatively measure the absorption coefficient for species of interest to the climate and atmospheric science communities. Because the system constant is known, in most applications the acoustic response of this instrument need not be calibrated against a sample of known optical density, a decided advantage in field applications. Routine enhancements, such as improved processing of the photoacoustic signal and higher laser beam power, should further increase the instrument's precision and sensitivity.

The effects of climate-forcing species on Earth's atmosphere are significant. For example, the 2007 Intergovernmental Panel on Climate Change (IPCC) report<sup>1</sup> concludes that anthropogenic greenhouse gases have resulted in a radiative forcing between 0.6 and  $2.4 \text{ W/m}^2$ . The IPCC report also estimates that the direct effect of aerosols on Earth's climate to be between  $-0.9$  and  $-0.1 \text{ W/m}^2$ . Many different analytical techniques are used to

study these species. Detection of greenhouse gases typically involves spectroscopic methods, such as nondispersive infrared<sup>2</sup> and tunable diode laser absorption spectroscopy.<sup>3</sup> The best instruments use advanced spectroscopic methods, such as cavity ring-down spectroscopy<sup>4,5</sup> (CRDS) or similar cavity-enhanced methods,<sup>6</sup> and measure gas concentrations with a relative standard uncertainty  $< 1\%$ . Determining the absorption coefficient for aerosols is complicated by the interplay between absorption and scattering. One approach is to obtain the absorption coefficient by subtracting the scattering coefficient, obtained from nephelometry, from the extinction coefficient (absorption + scattering), obtained from a cavity ring-down measurement, for example,<sup>7</sup> though the combined uncertainty in the deduced absorption coefficient can be substantial and the measurement can be subject to additional biases.<sup>8,9</sup>

Photoacoustic spectroscopy (PAS) is increasingly applied to the study of gases and aerosols and is gaining acceptance in these communities.<sup>10–18</sup> The appeal of PAS is that it measures the

- (2) Luft, K. F.; Schaefer, W.; Wiegleb, G. *Tech. Mess.* **1993**, *60*, 363–371.
- (3) Feher, M.; Martin, P. A. *Spectrochim. Acta, Part A* **1995**, *51*, 1579–1599.
- (4) Romanini, D.; Kachanov, A. A.; Sadeghi, N.; Stoeckel, F. *Chem. Phys. Lett.* **1997**, *264*, 316–322.
- (5) Romanini, D.; Kachanov, A. A.; Stoeckel, F. *Chem. Phys. Lett.* **1997**, *270*, 538–545.
- (6) O'Keefe, A.; Scherer, J. J.; Paul, J. B. *Chem. Phys. Lett.* **1999**, *307*, 343–349.
- (7) Pettersson, A.; Lovejoy, E. R.; Brock, C. A.; Brown, S. S.; Ravishankara, A. R. *J. Aerosol Sci.* **2004**, *35*, 995–1011.
- (8) Bond, T. C.; Anderson, T. L.; Campbell, D. *Aerosol Sci. Technol.* **1999**, *30*, 582–600.
- (9) Lack, D. A.; Cappa, C. D.; Cross, E. S.; Massoli, P.; Ahern, A. T.; Davidovits, P.; Onasch, T. B. *Aerosol Sci. Technol.* **2009**, *43*, 1006–1012.
- (10) Arnott, W. P.; Moosmuller, H.; Sheridan, P. J.; Ogren, J. A.; Raspert, R.; Slaton, W. V.; Hand, J. L.; Kreidenweis, S. M.; Collett, J. L. *J. Geophys. Res.* **2003**, *108*.
- (11) Gyawali, M.; Arnott, W. P.; Lewis, K.; Moosmuller, H. *Atmos. Chem. Phys.* **2009**, *9*, 8007–8015.
- (12) Haisch, C.; Beck, H.; Niessner, R. *Rev. Sci. Instrum.* **2003**, *74*, 509.
- (13) Lack, D. A.; Lovejoy, E. R.; Baynard, T.; Pettersson, A.; Ravishankara, A. R. *Aerosol Sci. Technol.* **2006**, *40*, 697–708.
- (14) Lack, D. A.; Quinn, P. K.; Massoli, P.; Bates, T. S.; Coffman, D.; Covert, D. S.; Sierau, B.; Tucker, S.; Baynard, T.; Lovejoy, E.; Murphy, D. M.; Ravishankara, A. R. *Geophys. Res. Lett.* **2009**, *36*.
- (15) Lewis, K.; Arnott, W. P.; Moosmuller, H.; Wold, C. E. *J. Geophys. Res.* **2008**, *113*.
- (16) Marinov, D.; Sigrist, M. W. *Photochem. Photobiol. Sci.* **2003**, *2*, 774–778.
- (17) Massoli, P.; Murphy, D. M.; Lack, D. A.; Baynard, T.; Brock, C. A.; Lovejoy, E. R. *Aerosol Sci. Technol.* **2009**, *42*, 1064–1074.

<sup>†</sup> Part of the special issue "Atmospheric Analysis as Related to Climate Change".

\* To whom correspondence should be addressed.

<sup>‡</sup> James Madison University.

<sup>§</sup> National Institute of Standards and Technology.

<sup>||</sup> University of Maryland.

(1) IPCC. *Climate Change 2007: The Physical Science Basis. Contribution of Working Group I to the Fourth Assessment Report of the Intergovernmental Panel on Climate Change*; Cambridge University Press: Cambridge, U.K., 2009.

absorption coefficient but not the extinction or scattering coefficients. While PAS does selectively measure absorption, it does so indirectly. First, the energy of the photon is deposited into the absorber and distributed through its internal degrees of freedom. Collisions between the excited absorber and the surrounding gas then convert this internal energy into translational energy. Finally, a microphone detects the pressure wave resulting from the localized heating of the bath gas. Often, this process takes place in an acoustic resonator where modulation of the incident light intensity at the resonant acoustic frequency amplifies the response.

Because of the confounding absorber- and matrix-specific processes involved in converting absorbed light into sound, absent independent knowledge of the cell constant, a photoacoustic spectrometer requires calibration in order to yield quantitative information. PAS calibrations usually involve a gaseous absorber.<sup>19,20</sup> The associated uncertainties are typically ~2% to ~10%. Most calibration techniques determine the microphone response for a sample of known absorption coefficient, tacitly assuming that thermalization of the internal energy in the excited species is efficient and fast. Lack et al.<sup>13</sup> developed a calibration protocol using O<sub>3</sub><sup>21</sup> and atomized nigrosin that achieved a combined relative uncertainty in the absorption coefficient of 1% to 2% for gas samples and <5% for aerosols. To achieve this, Lack et al.<sup>13</sup> linked the PAS measurement to a cavity ring-down spectrometer, an approach that, while successful, required considerable expertise and resources. Tian et al.<sup>22</sup> recently presented a PAS calibration procedure using the  $b^1\Sigma_g^+ \leftarrow X^3\Sigma_g^-(0,0)$  band of O<sub>2</sub>, for which spectroscopic parameters are known to better than 0.5%.<sup>23</sup> However, they did not consider the energy transfer processes involved in quenching the  $b^1\Sigma_g^+$  state, which resulted in a substantial error.<sup>24</sup>

Recently, we developed a photoacoustic resonator with a calculable cell constant.<sup>24</sup> Using air samples, we found the calculated and measured response functions to agree within 1%, which was within the combined relative uncertainty of the model and measurements. This means that the instrument response, embodied by the cell constant, can be discerned from first principles knowledge of the gas properties, cell geometry, and acoustic theory and does not necessarily require calibrations against reference samples with known optical properties.<sup>25–28</sup> This article presents new results that benchmark this instrument's performance when used for quantitative optical absorption measurements of species related to climate change. The concentration of CO<sub>2</sub> in laboratory air was measured with this instrument and

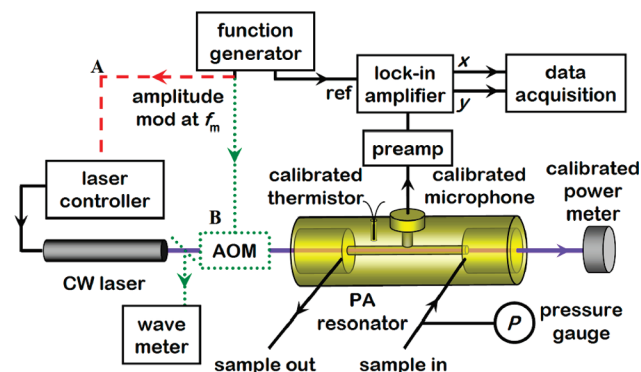


**Figure 1.** Schematic diagram for PAS absorption measurements of soot, O<sub>2</sub>, and CO<sub>2</sub>. Elements in path A (red dashed lines) correspond to soot measurements at  $\lambda = 405$  nm with direct intensity modulation. Elements in path B (green dotted lines) correspond to high-resolution O<sub>2</sub> and CO<sub>2</sub> gas-phase measurements near  $\lambda = 765$  and 1572 nm, respectively, using an acousto-optic modulator (AOM).

compared to measurements made using a cavity ring-down spectrometer. The enhanced absorption resulting from ultrathin (<5 nm), nonabsorbing coatings on nanoscale particles was measured to demonstrate the sensitivity of this instrument to the structure of aerosols. This article also presents an uncertainty analysis, reports detection limits for the existing spectrometer, and predicts the detection limits of an enhanced spectrometer.

## EXPERIMENTAL SECTION

**Instrumentation.** The apparatus shown in Figure 1 is similar to most PAS systems.<sup>29,30</sup> It is composed of a continuous-wave laser, an intensity modulator, an acoustic resonator,<sup>24</sup> a calibrated microphone, and a calibrated optical power meter. The data acquisition system includes a dual channel lock-in amplifier and electronics to handle instrument automation and data processing. As described by Gillis et al.,<sup>24</sup> the resonator consists of a 100 mm  $\times$  6 mm cylindrical duct (length  $\times$  diameter) positioned between two 50 mm  $\times$  30 mm cylindrical chambers. We measured the microphone sensitivity of 11.75(6) mV/Pa at 1640 Hz using a constant-amplitude sound source and a standard microphone. This sensitivity was characterized as a function of frequency and relative humidity.

The laser light intensity was sinusoidally modulated at the frequency  $f_m$ , using an acousto-optic modulator to match a selected resonance frequency,  $f_0$ , of the acoustic resonator. The lowest-order mode which efficiently couples to a modulated laser has a value of  $f_0 \sim 1640$  Hz in ambient air at 296 K.<sup>24</sup> However,  $f_0$  is proportional to the speed of sound in the gas (and therefore a function of gas temperature and composition). Thus, such shifts in  $f_0$  can alter the amplitude of the signal if  $f_m$  is not adjusted accordingly. To compensate for subsequent temperature-dependent changes in the PAS cell resonance frequency,<sup>16</sup> the control system can adjust the modulation frequency to remain on resonance by periodic scans of  $f_m$  about  $f_0$ . Alternatively, the acoustic response function can

- (18) Slowik, J. G.; Cross, E. S.; Han, J. H.; Davidovits, P.; Onasch, T. B.; Jayne, J. T.; Williams, L. R.; Canagaratna, M. R.; Worsnop, D. R.; Chakrabarty, R. K.; Moosmuller, H.; Arnott, W. P.; Schwarz, J. P.; Gao, R. S.; Fahey, D. W.; Kok, G. L.; Petzold, A. *Aerosol Sci. Technol.* **2007**, *41*, 295–314.
- (19) Adams, K. M.; Davis, L. I.; Japar, S. M.; Pierson, W. R. *Atmos. Environ.* **1989**, *23*, 693–700.
- (20) Arnott, W. P.; Moosmuller, H.; Rogers, C. F.; Jin, T. F.; Bruch, R. *Atmos. Environ.* **1999**, *33*, 2845–2852.
- (21) Orphal, J. J. *Photochem. Photobiol., A* **2003**, *157*, 185–209.
- (22) Tian, G. X.; Moosmuller, H.; Arnott, W. P. *Aerosol Sci. Technol.* **2009**, *42*, 1084–1090.
- (23) Long, D. A.; Havey, D. K.; Okumura, M.; Miller, C. E.; Hodges, J. T. J. *Quant. Spectrosc. Radiat. Transfer* **2010**, *111*, 2021.
- (24) Gillis, K. A.; Havey, D. K.; Hodges, J. T. *Rev. Sci. Instrum.* **2010**, *81*, 064902.
- (25) Arnott, W. P.; Moosmuller, H.; Walker, J. W. *Rev. Sci. Instrum.* **2000**, *71*, 4545–4552.
- (26) Petzold, A.; Niessner, R. *Appl. Phys. B: Lasers Opt.* **1996**, *63*, 191–197.
- (27) Schafer, S.; Miklos, A.; Hess, P. *Appl. Opt.* **1997**, *36*, 3202–3211.
- (28) Miklos, A.; Hess, P.; Bozoki, Z. *Rev. Sci. Instrum.* **2001**, *72*, 1937–1955.

(29) Claspy, P. C. In *Optoacoustic Spectroscopy and Detection*; Pao, E. Y.-H., Ed.; Academic Press: New York, 1977; pp 133–166.

(30) Rosencwaig, A. *Photoacoustics and Photoacoustic Spectroscopy*; John Wiley & Sons: New York, 1980.

be used to account for small temperature changes using precision temperature measurements and the known gas properties. We found that the latter method improved the precision of our measurements by as much as 40% for temperature excursions,  $\Delta T$  of 1–2 K, without the need to rescan the acoustic resonance.

After the laser modulation frequency is tuned to the peak of the acoustic resonance, the laser wavelength must be matched to a spectral region of optical absorption to probe an analyte of interest. For aerosol particles this is generally simple since absorption features are, for the most part, spectrally broad. In the case of a greenhouse gases, spectra are usually characterized by narrow transitions with characteristic widths that are typically  $<0.2 \text{ cm}^{-1}$ . Resolving these spectra requires that the probe laser be single mode and tunable. In practice, the laser wavelength should be scanned over one or more absorption transitions to yield a spectrum that can be fit using line-by-line models. This spectrally resolved method requires an accurate determination of the steps in laser wavelength. Alternatively, gas concentration can be determined by collecting PAS data at fixed wavelength (usually at the peak of a dominant transition) and modeling the local absorption coefficient.

Assuming a molecular relaxation efficiency of unity, the fundamental relationship in PAS for obtaining the absorption coefficient is<sup>24,28</sup>

$$\alpha = \frac{R_{\text{PAS}}}{W_{\text{pp}} C_c \beta_m} \quad (1)$$

where  $R_{\text{PAS}}$  is the amplitude of the microphone signal measured by a phase-sensitive (lock-in) detector that is synchronized to the modulation frequency,  $W_{\text{pp}}$  is the peak-to-peak laser power (i.e., the maximum-to-minimum of the modulated component of the power),  $C_c$  is the modeled cell constant, and  $\beta_m$  is the microphone sensitivity. We note that all three quantities in the denominator in eq 1 are frequency dependent and must be evaluated at the modulation frequency,  $f_m$ .

**Measurements.** We performed experiments on a few select systems to evaluate instrument performance. First, measurements were made on  $\text{O}_2$  in laboratory air, 20.95% by volume,<sup>31</sup> at 300.0 K and 100.8 kPa. Additional measurements were made on samples of humidified  $\text{CO}_2$  at 298.9 K and 99.88 kPa as well as trace  $\text{CO}_2$  in laboratory air. Here we utilized tunable single-mode external cavity diode lasers centered at  $\lambda = 765 \text{ nm}$  for  $\text{O}_2$  and  $\lambda = 1590 \text{ nm}$  for  $\text{CO}_2$ . To measure the wavenumber of the laser beam, we used a wavemeter with a standard uncertainty of  $0.002 \text{ cm}^{-1}$ . For these gases, we also exploited the well-known line intensities, self- and air-broadening parameters, and Dicke narrowing parameters of Robichaud et al.<sup>32</sup> and Havey et al.<sup>33</sup> for the  $\text{O}_2$  A-band as well as line intensities and broadening parameters of Toth et al.<sup>34</sup> for  $\text{CO}_2$ . We used

Galatry profiles<sup>35</sup> to fit the measured PAS  $\text{O}_2$  A-band spectra. Currently, contributions to the measured absorption coefficients from higher-order line shape effects, such as line mixing, are assumed to be small relative to the 1% combined uncertainty in the instrument response<sup>24</sup> and are not incorporated into this data analysis.

PAS measurements were also made on flowing samples of soot particles carried by dry air. We measured size-selected soot particles having mean mobility diameters of 100, 150, and 200 nm. Details on the experimental apparatus used to generate and classify the soot are described by Kim et al.<sup>36</sup> An ethylene fueled Santoro-style diffusion flame<sup>37</sup> was used to generate soot particles. Soot was then transported to a differential mobility analyzer (DMA) for size characterization and classification. Prior to passing through the DMA, the soot particles passed through an aerosol neutralizer containing  $^{210}\text{Po}$  in order to place an equilibrium charge of +1 on the particles.<sup>38</sup> A DMA separates particles according to their mobility by balancing the drag force and the electrical force on the particles. In scanning mode, the DMA measures the particle size distribution. In selection mode, the DMA selects a narrow size distribution of particles. For the present work, the DMA was set to select 100, 150, or 200 nm mobility diameter soot particles. After passing through the DMA, soot particles were analyzed with the photoacoustic spectrometer using a  $\lambda \sim 405 \text{ nm}$  multimode diode laser and then sent to a condensation nuclei particle counter (CPC) to measure the number density. We corrected the measured number density  $N_m$  to account for shielding effects in the condensation particle counter<sup>39</sup> that occur when two or more particles arrive simultaneously. This coincidence correction is modeled as  $N_c/N_m = \exp(-N_c q t_m)$ , where  $N_c$  is the coincidence-corrected particle number density,  $q$  is the volumetric flow rate, and  $t_m$  is the measurement time for the CPC. The coincidence correction was between 2.6% and 8.2% for the measurements presented here. The DMA was calibrated with NIST SRM 1964 (60 nm polystyrene latex spheres) which has a relative combined standard uncertainty in mobility diameter of 0.5%.<sup>40</sup>

We measured the absorption of both bare soot particles and soot particles coated by an optically nonabsorbing layer of liquid dibutyl phthalate (DBP). DBP is a surrogate for species such as  $\text{H}_2\text{SO}_4(\text{aq})$ , which can coat soot particles found in the atmosphere. The size-selected bare soot particles, acting as condensation nuclei, were sent through a heated coating chamber filled with DBP at its saturated vapor pressure. This process resulted in DBP-coated soot particles with a core–shell structure. The coating thickness was varied by adjusting the temperature of the coating chamber. With the use of this technique, the minimum achievable coating thickness was estimated to be  $<5 \text{ nm}$ , as discussed below.

(35) Galatry, L. *Phys. Rev.* **1961**, *122*, 1218.

(36) Kim, S. H.; Fletcher, R. A.; Zachariah, M. R. *Environ. Sci. Technol.* **2005**, *39*, 4021–4026.

(37) Santoro, R. J.; Semerjian, H. G.; Dobbins, R. A. *Combust. Flame* **1983**, *51*, 203–218.

(38) Wiedensohler, A. *J. Aerosol Sci.* **1988**, *19*, 387–389.

(39) Gebhart, J. In *Aerosol Measurements: Principles, Techniques, and Applications*; Baron, P. A.; Willeke, K., Eds.; Wiley-Interscience, Inc.: New York, 2001.

(40) Mulholland, G. W.; Donnelly, M. K.; Hagwood, C. R.; Kukuck, S. R.; Hackley, V. A.; Pui, D. Y. H. *J. Res. Natl. Inst. Stand. Technol.* **2006**, *111*, 257–312.

(31) Seinfeld, J. H.; Pandis, S. N. *Atmospheric Chemistry and Physics: From Air Pollution to Climate Change*; Wiley: New York, 1998.

(32) Robichaud, D. J.; Hodges, J. T.; Brown, L. R.; Lisak, D.; Maslowski, P.; Yeung, L. Y.; Okumura, M.; Miller, C. E. *J. Mol. Spectrosc.* **2008**, *248*, 1–13.

(33) Havey, D. K.; Long, D. A.; Okumura, M.; Miller, C. E.; Hodges, J. T. *Chem. Phys. Lett.* **2009**, *483*, 49–54.

(34) Toth, R. A.; Brown, L. R.; Miller, C. E.; Devi, V. M.; Benner, D. C. *J. Quant. Spectrosc. Radiat. Transfer* **2008**, *109*, 906–921.

## RESULTS AND DISCUSSION

**Measurement Uncertainty.** Relevant performance criteria for the PAS spectrometer are its (1) accuracy, the relationship between the mean value of a set of measurements and the true value; (2) precision, the variation within a set of independent measurements, which is linked to the detection limit; and (3) combined (total) uncertainty,  $u_c(y)$ , a numerical value which characterizes the range of values that can be attributed to the measurand,  $y$ , within a given confidence interval. The components of  $u_c(y)$  include type *A* uncertainties, which are those evaluated by statistical methods, and type *B* uncertainties, which are those evaluated by other nonstatistical means. The statistically independent component uncertainties are added in quadrature to give  $u_c(y)$ . In this work, the Allan deviation (see below) is a type *A* uncertainty quantifying the precision with which  $R_{\text{PAS}}/W_{\text{pp}}$  (and hence  $\alpha$  through eq 1) can be measured. The dominant type *B* effects in the measurand  $\alpha$  arise from uncertainties in the cell constant, microphone sensitivity, and radiometric laser power meter calibration, whose relative combined standard uncertainties are  $\sim 1\%$ . Apart from characterization of these quantities, in order to measure  $\alpha$  we do not need to perform other instrumental calibrations or utilize other analytical techniques. In our gas-phase measurements of absorber number density, which are derived from  $\alpha$ , there are two additional type *B* effects. These include systematic uncertainties in measurements of sample pressure and temperature, for which the relative combined standard uncertainties are  $\sim 0.1\%$ . Analogously for aerosols, independent measurements of the particle number density are required for PAS determination of particle cross section.

**PAS System Calibration and Measurement Accuracy.** There have been numerous studies describing alternative methods for calibrating the absolute response of PAS spectrometers to determine the type *B* uncertainty. However, only a relatively small number have explicitly compared the calibrated and calculated responses for a specific acoustic resonator. In an aerosol study, Petzold and Niessner<sup>26</sup> used diesel soot as a sample of known absorption coefficient and compared the measured PAS signal to modeled values which were based on the resonator geometry, gas properties, and microphone sensitivity. Similarly, Arnott et al.<sup>25</sup> measured and modeled a PAS system using samples of  $\text{NO}_2$  gas as a reference absorber. In both of these studies, standard uncertainties in the sample absorption coefficient precluded validation of the PAS model to better than 10%. In contrast, we have significantly reduced the discrepancy between the measured and calculated acoustic response to be of the order of 1%. With this level of uncertainty, we propose that the calculated system response could be used to realize traceability in PAS measurements of absorption coefficient for both gases and aerosols.

We found little or no change in the PAS system response upon long-term exposure to soot aerosols. After conducting a series of PAS measurements on soot aerosols over the course of more than 1 year, the system response (based on comparison to  $\text{O}_2$  *A*-band gas phase spectra) was consistent to within 0.5%. These tests illustrate that fouling of PAS system by soot aerosols and concomitant changes to the system response can be avoided.

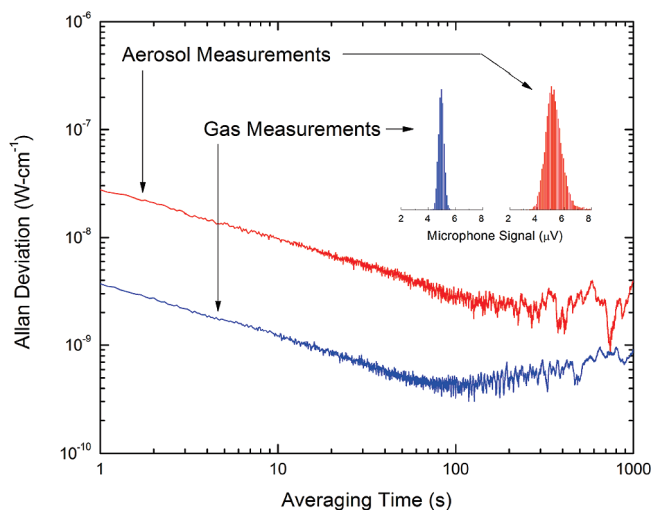


**Figure 2.** Power normalized Allan deviations are shown for absorption measurements at line center an  $\text{O}_2$  *A*-band transition (lower, blue) and for  $100 \pm 1$  nm mobility diameter soot particles (upper, red). Noise distributions are shown in the inset.

**Detection Limits.** The ultimate level to which one can measure absorption coefficients is limited by the PAS system type *A* uncertainties, which can be quantified by the Allan deviations<sup>41</sup> shown Figure 2. To obtain this Allan deviation we measured an absorption signal in ambient air (300 K, 100.8 kPa) by probing the peak of the  $^P(9)$   $\text{O}_2$  *A*-band transition at  $13\,091.710\text{ cm}^{-1}$ . For this measurement  $W_{\text{pp}} \sim 3$  mW. Aerosol measurements were made on a flowing stream of  $100 \pm 1$  nm mobility diameter soot particles with  $W_{\text{pp}} \sim 200$  mW. In both cases, optical absorption was measured for 2 h at uniform intervals of 0.1 s. For a 60 s averaging time, the detection limits, given by the product of power and absorption coefficient,  $\alpha_{\text{min}}W_{\text{pp}}$ , were measured to be  $4 \times 10^{-10}\text{ W cm}^{-1}$  for the  $\text{O}_2$  *A*-band and  $2 \times 10^{-9}\text{ W cm}^{-1}$  for soot particles. The minimum in the Allan deviation corresponds to the optimal short-term averaging time. It occurs between 50 and 100 s for measurements of the  $\text{O}_2$  *A*-band and between 100 and 300 s for soot particles. The differences in the Allan deviation plots are most likely caused by two factors: (1) increased random noise generated by a fluctuating aerosol source (see Figure 2 inset) and (2) the relatively narrow  $\text{O}_2$  absorption lines compared to the spectrally broad aerosol absorption signatures. For soot aerosols, the latter effect reduces sensitivity to laser frequency drift and allows for longer averaging times. However for all the gas and aerosol measurements reported here, we chose a 60 s averaging time.

A comparison of detection limits for a selection of PAS instruments in the literature is shown in Table 1. The sensitivity of our spectrometer compares favorably against numerous groups utilizing PAS for an array of different applications.<sup>13,20,42–45</sup> Table 1 shows that PAS measurements in gas samples have detection limits approximately 10 times lower than those made on aerosol systems; a difference which we assign to the complexity and variability of aerosol samples. Consequently, gas sample perfor-

(41) Allan, D. W. *Proc. IEEE* **1966**, *54*, 221.

**Table 1. Comparison of PAS Detection Limits**

ref	year	$\alpha_{\min} W_{pp} (t_{\text{avg}})^{1/2}$ (nW cm <sup>-1</sup> Hz <sup>-1/2</sup> )	
		gas	aerosol
Pushkarsky et al. <sup>a, 45</sup>	2003	2.2	
Miklos et al. <sup>44</sup>	2006	3.3	
Kosterev et al. <sup>43</sup>	2005	5.4	
Arnott et al. <sup>42</sup>	2006		20
Lack et al. <sup>b, 13</sup>	2006		31
Arnott et al. <sup>20</sup>	1999		68
present study	2010	3.1	15

<sup>a</sup> Authors understate their capabilities. <sup>b</sup> Detection limit calculation assumes a peak-to-peak power of 8 W with square-wave modulation and is converted to a standard uncertainty for comparison with the present work and other published values.

mance metrics should not be used for predicting aerosol sample measurement capabilities and vice versa.

**Measurement of CO<sub>2</sub>.** We performed two experiments: the first involved measurements of CO<sub>2</sub> at high concentration and hence high PAS signal-to-noise ratio; the second involved PAS and CRDS measurements of CO<sub>2</sub> in ambient laboratory air. Both the PAS and CRDS measured absorption by probing only line center and baseline points in the wings of the absorption lines. We modeled the spectra using the line parameters of Toth et al.<sup>34</sup> and corrected the data to account for the temperature-dependence of the line intensity.

In the first experiment we used PAS to evaluate instrument performance on a gas other than O<sub>2</sub>. To this end, we measured absorption by humidified CO<sub>2</sub> (20–30% RH) at 298.9 K and 99.88 kPa. We probed the R22e and R20e transitions at 6363.726 and at 6362.504 cm<sup>-1</sup>, respectively, within the (30°1) ← (00°1) combination band. The signal-to-noise level, defined as the peak absorption divided by the standard deviation of the spectrally detuned baseline, was ~5000:1. This result is in good agreement with the type A relative uncertainty of ~6000:1, based upon the ratio of the peak absorption to the Allan deviation. Absorption coefficient measurements for two transitions were taken over a 1 h period. The time series of the reduced measurements for each transition is shown in Figure 3. Measurements and published values agree to within their combined uncertainties. Nevertheless, these data exhibit a small time-dependent drift which we assign to subtle changes in the PAS-cell window transmittance. This effect was unique to the windows used for this wavelength region and was caused by variation in the humidity level of the gas sample. We find that the relative standard deviation of each ensemble is ~0.4%, which is about ~20 times greater than the expected type A uncertainty based on the Allan deviation. These results illustrate the exceptionally high sensitivity of the PAS measurement for measuring changes in gas concentration.

In the second experiment, we investigated the precision and accuracy of the PAS as an atmospheric CO<sub>2</sub> monitoring device

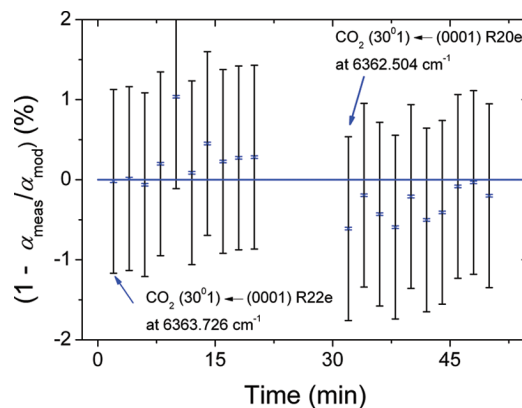


**Figure 3.** Differences between measured and modeled absorption coefficients for two CO<sub>2</sub> transitions. Error bars correspond to relative combined standard uncertainties (outer bars) containing contributions from type A components (inner bars) and type B uncertainties in system constant, temperature, pressure, and power.

by comparison with a CRDS spectrometer. The expected relative precision of the PAS measurement is  $\alpha_{\min}/\alpha_{\text{peak}} = 0.303$ . Here  $\alpha_{\min} = 2 \times 10^{-7}$  cm<sup>-1</sup> is based on  $W_{pp} = 2$  mW and  $\alpha_{\text{peak}} = 6.6 \times 10^{-7}$  cm<sup>-1</sup> is the absorption coefficient at the peak of the (30°1) ← (00°1) R22e transition at a pressure of 101 kPa.<sup>34</sup> This estimate also assumes a nominal CO<sub>2</sub> molar fraction,  $x_{\text{CO}_2}$ , of 385 μmol mol<sup>-1</sup>, which is close to the present global average value. (Note, however, that measured values can be expected to be larger than the global average because of the urban dome effect<sup>46</sup>). We took three sets of 10 PAS measurements,  $n_m = 30$ , over the course of several days, and we obtained a mean value of 466 μmol mol<sup>-1</sup> for  $x_{\text{CO}_2}$ , with a relative standard deviation of  $u_r(x_{\text{CO}_2}) = 6.9\%$ . This result is in good agreement with the expected value of 5.5% given by  $u_r(x_{\text{CO}_2}) = (\alpha_{\min}/\alpha_{\text{peak}}) n_m^{-1/2}$ .

We took several sets of CRDS measurements of CO<sub>2</sub> in laboratory air, although these measurements were made on different days than the PAS experiments. The CRDS measurements were made at a pressure of 26.3 kPa, to minimize the effects of line blending and to ensure a well-defined baseline. The ensemble of CRDS measurements yielded an average  $x_{\text{CO}_2}$  of 463 μmol mol<sup>-1</sup> with a standard deviation of 15 μmol mol<sup>-1</sup>. The type A uncertainty of these measurements was driven by the slight day-to-day variations in the laser detuning about line center, which were limited by the 0.001 cm<sup>-1</sup> wavenumber resolution of the wavemeter. For the known spectrum line profile, this uncertainty in laser wavenumber corresponds to a relative variation in absorption coefficient of ~3%, nearly equaling the relative standard deviation of the ensemble of CRDS measurements. These ring-down data indicate that daily variations in the ambient CO<sub>2</sub> molar fraction were less than ~5 μmol mol<sup>-1</sup> and therefore had little bearing on the intercomparison.

In summary, we find that the PAS and CRDS measurements of CO<sub>2</sub> agreed to within their relative combined standard uncertainties, with their mean values differing by less than 1%. Moreover the long-term precision of the PAS measurements was consistent with the type A uncertainties given by our Allan deviation analysis.

(42) Arnott, W. P.; Walker, J. W.; Moosmuller, H.; Elleman, R. A.; Jonsson, H. H.; Buzorius, G.; Conant, W. C.; Flagan, R. C.; Seinfeld, J. H. *J. Geophys. Res.* **2006**, *111*.

(43) Kosterev, A. A.; Tittel, F. K.; Serebryakov, D. V.; Malinovsky, A. L.; Morozov, I. V. *Rev. Sci. Instrum.* **2005**, *76*.

(44) Miklos, A.; Pei, S. C.; Kung, A. H. *Appl. Opt.* **2006**, *45*, 2529–2534.

(45) Pushkarsky, M. B.; Webber, M. E.; Patel, C. K. N. *Appl. Phys. B: Lasers Opt.* **2003**, *77*, 381–385.

(46) Jacobson, M. Z. *Environ. Sci. Technol.* **2010**, *44*, 2497–2502.

**Absorption Measurements of Soot Aerosols.** The radiative properties of soot particles are atmospherically relevant but cannot be readily predicted from first principles. Likewise the required optical measurements on soot are challenging. Two of the most important of these properties include the wavelength-dependent absorption and scattering cross sections. Both models and measurements must account for the fact that soot particles can vary in size, shape, mixing state, and chemical composition depending on how they are generated. These aspects directly affect optical properties and consequently measurements are required over a wide range of conditions. Since PAS provides a direct measure of absorption coefficient, it has been used to determine absorption cross section for an absorbing aerosol such as soot,<sup>12</sup> when used in conjunction with particle counting methods.

To address these measurement requirements, instruments for quantifying aerosol radiative properties need to have certain attributes: (1) rapid response time, (2) sensitivity to distinguish changes in size, shape, and chemical composition, (3) durability, and (4) capability to operate under convenient conditions (e.g., ambient pressure and temperature). We performed two experiments to evaluate how our PAS spectrometer performs in this context for measurements of absorbing aerosols. The first experiment was a study of the short- and long-term stability of the uncoated particle stream, which includes the soot generation and size selection instrumentation. In the second experiment, we studied DBP-coated soot to quantify the minimum detectable coating thickness and to look for predicted coating-induced enhancement in particle absorption cross section.

In the first experiment, we investigated size-selected bare soot particles having a mobility diameter,  $d_m = 100$  nm. We monitored the PAS and CPC signals for a period of 5 h and repeated this measurement four times over the span of several days. Figure 4 shows the time evolution of these data on two different days, represented by the upper and lower traces in each panel. Inspection of the PAS and CPC data shown in parts a and b of Figure 4, respectively, indicates that there are strong correlations between these measured quantities on a given day. Variations in the PAS signal are dominated by relatively large fluctuations and drift in  $N_c$ , whereas changes in the laser power are negligible by comparison (Figure 4c). In Figure 4d, we show the soot particle absorption cross section,  $\sigma = \alpha/N_c$ , where  $\alpha$  is obtained from eq 1. It is apparent that  $\sigma$  exhibits much less variability within a given day than does  $N_c$ . For each 5 h data set, the type A relative standard deviation in  $\sigma$  is  $\sim 1.5\%$ , and for short-term times scales (0.1 h), this value is  $< 1\%$ . However, considering all four data sets together, the relative day-to-day variation in  $\sigma$  was  $\sim 10\%$ . There are a number of possible reasons for the observed variation in  $\sigma$ . These include irreproducibility in the morphology, shape and composition of the flame-generated soot and effects in the charging and DMA systems that alter the size distribution of the particles.

The soot particles comprise agglomerates of nearly spherical primary particles  $\sim 20$  nm in diameter. Because of their complex shape, the mobility diameter measured by the DMA is different than the sphere-equivalent particle diameter,  $d_{se}$ , of the agglomerate. For the 100 nm mobility diameter soot particles, we estimate  $d_{se} = 70$  nm. Assuming a soot complex refractive

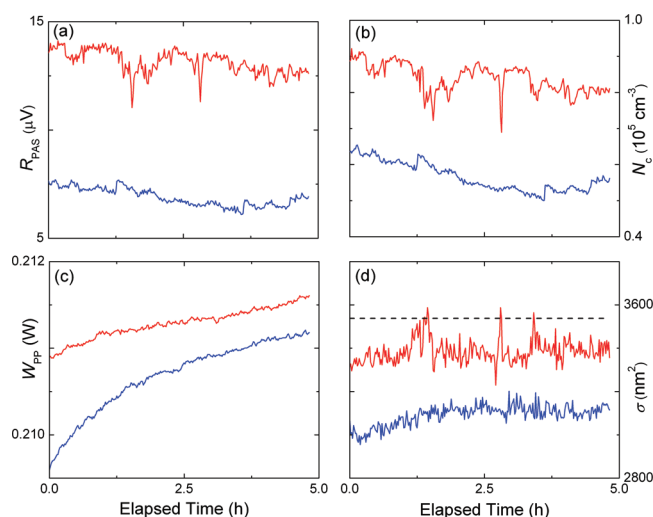


**Figure 4.** Time dependence of PAS and CPC measurements for two measurement sets [upper (red) and lower (blue) traces] obtained on different days and for  $d_{se} = 70$  nm: (a)  $R_{PAS}$ ; (b)  $N_c$ ; (c)  $W_{PP}$ ; and (d)  $\sigma = R_{PAS}/(C_d\beta_m W_{PP} N_c)$ , where  $C_d\beta_m = 18.7$  V cm  $W^{-1}$ . The dashed horizontal line in panel d corresponds to the calculated absorption cross section.

index,  $m_{soot} = 1.55 + 0.8i$ , in the Rayleigh limit the monomer absorption cross section per volume is  $0.0195$  nm $^{-1}$ , yielding an aggregate absorption cross section  $\sigma = 3542$  nm $^2$ . The measured and calculated values of the soot absorption cross section (Figure 4d) agree.

In a second experiment, we measured the change in absorption (relative to the bare particle case) associated with thin layers of DBP on 150 and 200 nm mobility diameter soot particles. The sphere-equivalent diameters and absorption cross sections for these two cases are given in Table 2. Several groups have now quantified increased absorption of soot particles from the presence of a nonabsorbing coating.<sup>9,47–49</sup> Here, we coated soot with the smallest amount of DBP that the coating chamber could provide and measured the fractional change in the absorption cross section caused by the nonabsorbing coating. TEM micrographs of DBP-coated soot particles indicate that the coating process restructured the soot into a more compact form, producing a core–shell configuration. The PAS results are shown in Figure 5 and indicate that in both cases a change in absorption cross section was readily observed. We performed Lorenz–Mie theory (LMT) calculations for layered spheres in order to estimate the coating thickness for these measurements and to calculate a minimum detectable shell thickness that could be compared with our experimental results.<sup>50</sup> LMT predicts the absorption cross section of a radially symmetric core–shell particle in terms of the core diameter,  $d_c$ , the coating thickness,  $t_c$ , and the complex refractive indices of the core,  $m_1$ , and coating,  $m_2$ . We assumed  $m_1 = m_{soot}$  and  $m_2 = 1.5 + 0i$ . In the thin coating limit,  $t_c < d_c/2$ , LMT gives  $\Delta\sigma \approx$

(47) Xue, H. X.; Khalizov, A. F.; Wang, L.; Zheng, J.; Zhang, R. Y. *Phys. Chem. Chem. Phys.* **2009**, *11*, 7869–7875.

(48) Shiraiwa, M.; Kondo, Y.; Iwamoto, T.; Kita, K. *Aerosol Sci. Technol.* **2010**, *44*, 46–54.

(49) Zhang, R. Y.; Khalizov, A. F.; Pagels, J.; Zhang, D.; Xue, H. X.; McMurry, P. H. *Proc. Natl. Acad. Sci. U.S.A.* **2008**, *105*, 10291–10296.

(50) Bohren, C. F.; Huffman, D. R. *Absorption and Scattering of Light by Small Particles*; Wiley-VCH: Weinheim, Germany, 2004.

**Table 2. Soot Cross Sections and DBP Coating Thicknesses**

$d_m$ (nm)	$d_{se}$ (nm)	$\sigma$ (nm <sup>2</sup> )	$\Delta\sigma/\sigma$ (%)	std deviation (%)	$d\sigma/dt_c$ (nm <sup>2</sup> /nm)	$\Delta t_c$ (nm)	$\Delta t_{c,min}$ (nm) <sup>a</sup>	$\Delta t_{c,min}$ (nm) <sup>b</sup>
100	70.2	3542						
150	94.2	8549	5.7	0.9	110	4.4	0.7	0.13
200	107.7	12760	4.3	1.1	144	3.8	1.0	0.10

<sup>a</sup> On the basis of the measured standard deviation in Figure 5. <sup>b</sup> On the basis of the aerosol Allan deviation in Figure 2.

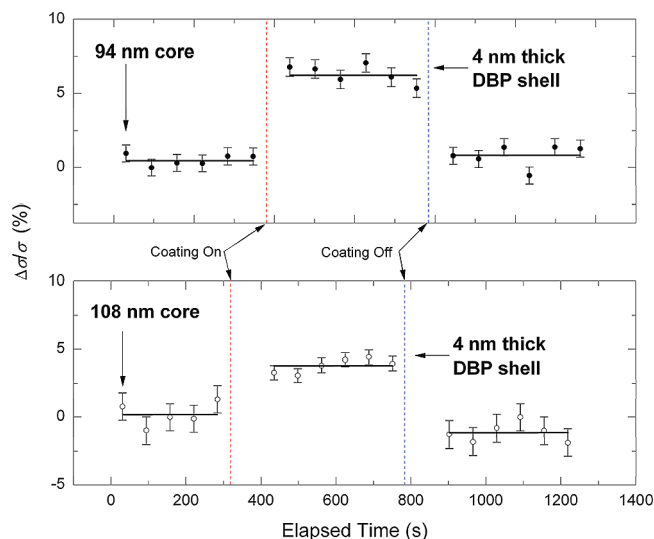


**Figure 5.** Measured changes in absorption cross section for soot particles of diameters,  $d_{se} = 94$  and  $108$  nm coated with DBP. Uncertainties correspond to 1 standard deviation in measured  $\Delta\sigma$ .

$t_c \kappa(m_1, m_2) d_c^2$ , where  $\Delta\sigma$  is the change in the absorption cross section relative to that of the bare core particle and  $\kappa$  is a constant that depends only on the two indices of refraction. In the present case  $\kappa = 1.24 \times 10^{-2} \text{ nm}^{-1}$ . If we denote  $\Delta\sigma_{min}$  as the minimum detectable change in  $\sigma$ , it follows that the minimum detectable change in the coating thickness is  $\Delta t_{c,min} = \Delta\sigma_{min}/(\kappa d_c^2) = \alpha_{min}/(N_c \kappa d_c^2)$ . From the known absorption cross sections and the measured fractional changes in absorption cross section ( $\sim 5.7\%$  and  $\sim 4.3\%$ ) shown in Figure 5, we estimate coating thicknesses of  $\sim 4$  nm for both cases. Given the precision of the measurements shown in Figure 5 ( $\sim 1\%$  relative std deviation in  $\sigma$ ), these results show that  $\Delta t_{c,min} \sim 0.7\text{--}1$  nm, whereas using the value of  $\Delta\sigma_{min}$  based on Allan deviation yields  $\Delta t_{c,min} \sim 0.1$  nm. These results are summarized in Table 2.

In contrast, previous PAS results demonstrated enhanced soot particle absorption only for relatively thick nonabsorbing coatings. Specifically, Shiraiwa et al.<sup>48</sup> saw amplification effects on coated BC (black carbon) particles for coated particles with diameters 20% or greater than those of the cores, and Slowik et al.<sup>18</sup> state that “. . . organic coatings on the order of  $\sim 10$  nm do not affect the BC readings.” In the present study, we have shown that the effect of nonabsorbing layers that are much less than 5 nm thick can be measured using PAS.

Soot particles in the atmosphere are also often found to be coated with a thin layer of optically absorbing organic material. Commonly observed compounds include polycyclic aromatic hydrocarbons (PAHs). Considering anthracene (complex refrac-

tive index at  $\lambda = 500$  nm of  $m_2 = 3.5 + 0.88i$ )<sup>51</sup> as a representative PAH and assuming  $N_c = 10^5 \text{ cm}^{-3}$ ,  $W_{PP} = 200$  mW, and a 100 nm diameter soot core, we estimate that one could observe changes in the absorption cross section caused by layers that are 2 nm thick or less.

## CONCLUSIONS

We have experimentally characterized the performance of the PAS technique in the context of some representative atmospheric applications. For measurements of  $\text{CO}_2$ , we demonstrated the ability to do precise and accurate spectroscopic measurements by comparison with known  $\text{CO}_2$  line parameters.<sup>34</sup> We also implemented a proof-of-concept experiment that confirmed the potential use of PAS as a point-source greenhouse gas sensor. We demonstrated detection limits of the absorption coefficient (averaging time of 60 s) to be  $4 \times 10^{-10} \text{ W cm}^{-1}$  for a gas and  $2 \times 10^{-9} \text{ W cm}^{-1}$  for a soot aerosol. The detection limit for soot was determined primarily by generation, classification, and measurement of the particle number density. We measured absorption cross sections of 100 nm diameter soot particles, obtained type A relative standard uncertainties  $<1\%$  and  $<1.5\%$  over short- (1 h) and long-term (5 h) time scales, respectively, and we observed enhanced absorption for 150 and 200 nm diameter soot particles with a nonabsorbing layer  $<5$  nm thick. We conclude that a PAS spectrometer of this type, which includes a first-principles theoretical model to underpin the system cell constant, is well-suited for measurements of atmospherically relevant systems. The 1% relative combined standard uncertainty of the calibrated and modeled resonator response<sup>24</sup> potentially enables a PAS-based sensor to compete directly with existing state-of-the-art spectroscopic greenhouse gas detectors.

Our analysis suggests that substantial reduction of PAS detection limits and faster response times can be achieved by increasing the signal (with higher power lasers and/or cavity-enhanced methods<sup>52</sup>), reducing signal noise, or both. Noise reduction is possible using advanced microphone technology with a pressure-equivalent noise figure as low as  $<3 \mu\text{Pa Hz}^{-1/2}$ .<sup>53</sup> Ultimate detection limits for sample absorption coefficient may be at the  $10^{-11} \text{ cm}^{-1}$  level or below. We base this estimate on a 2-fold reduction in microphone noise and the relatively modest assumption of 20 W of circulating power in an optical resonator with a finesse of  $\sim 300$  (mirror reflectivity of 0.99) pumped by a 0.5 W laser. Combined with robustly engineered controls for temperature and pressure, a PAS spectrometer with

(51) Yakuphanoglu, F.; Arslan, M. *Opt. Mater.* **2004**, *27*, 29–37.

(52) Rossi, A.; Buffa, R.; Scotoni, M.; Bassi, D.; Iannotta, S.; Boschetti, A. *Appl. Phys. Lett.* **2005**, *87*.

(53) Hall, N. A.; Okandan, M.; Littrell, R.; Bicen, B. B.; Degertekin, F. L. *J. Acoust. Soc. Am.* **2007**, *122*, 2031–2037.

these attributes should enable a wide variety of sensitive and accurate measurements of optical absorption. Further, by combining of PAS-based absorption with extinction measurements, one can determine the total scattering coefficient. This approach may provide an attractive alternative to nephelometry for determining particle albedo, especially for large and/or complicated scattering particles that exhibit moderate to significant levels of absorption. Utilizing these approaches in tandem may open up new ways of probing particle interfaces to better understand problems relating to atmospheric and climate chemistry.

#### **ACKNOWLEDGMENT**

D. K. Havey received support from the National Research Council as a postdoctoral fellow at NIST. K. L. Plath is thanked for providing assistance with CRDS measurements of CO<sub>2</sub> concentrations in laboratory air.

Received for review May 25, 2010. Accepted August 23, 2010.

AC101366E